Earth Surface Processes and Landforms
Earth Surf. Process. Landforms **33**, 1192–1209 (2008)
Published online 12 October 2007 in Wiley InterScience
(www.interscience.wiley.com) **DOI:** 10.1002/esp.1607

Relation between flow, surface-layer armoring and sediment transport in gravel-bed rivers

John Pitlick,[1]* Erich R. Mueller,[1] Catalina Segura,[1] Robert Cress[2] and Margaret Torizzo[3]
[1] *Department of Geography, University of Colorado, Boulder, CO, USA*
[2] *Electrical Systems Consultants, Fort Collins, CO, USA*
[3] *Watershed Consulting Associates, Stowe, VT, USA*

**Correspondence to: John Pitlick, Department of Geography, Box 260, University of Colorado, Boulder, CO 80309, USA.*
E-mail: pitlick@colorado.edu

Received 10 May 2006;
Revised 10 July 2007;
Accepted 18 July 2007

Abstract

This study investigates trends in bed surface and substrate grain sizes in relation to reach-scale hydraulics using data from more than 100 gravel-bed stream reaches in Colorado and Utah. Collocated measurements of surface and substrate sediment, bankfull channel geometry and channel slope are used to examine relations between reach-average shear stress and bed sediment grain size. Slopes at the study sites range from 0·0003 to 0·07; bankfull depths range from 0·2 to 5 m and bankfull widths range from 2 to 200 m. The data show that there is much less variation in the median grain size of the substrate, D_{50s}, than there is in the median grain size of the surface, D_{50}; the ratio of D_{50} to D_{50s} thus decreases from about four in headwater reaches with high shear stress to less than two in downstream reaches with low shear stress. Similar trends are observed in an independent data set obtained from measurements in gravel-bed streams in Idaho. A conceptual quantitative model is developed on the basis of these observations to track differences in bed load transport through an idealized stream system. The results of the transport model suggest that downstream trends in total bed load flux may vary appreciably, depending on the assumed relation between surface and substrate grain sizes. Copyright © 2007 John Wiley & Sons, Ltd.

Keywords: bedload; armoring; substrate

Introduction

The sediment supplied to high gradient streams often consists of a widely graded mix of grain sizes, ranging from sand to large boulders. In many streams the sediment supplied is sorted vertically into a coarse fraction that is retained on the bed surface (the armor layer) and a fine fraction that goes into temporary storage in the bed (the substrate). The armor layer contains a high proportion of coarse clasts and is typically about as thick as the diameter of the largest grains supplied to the channel. The substrate contains a high proportion of sand and granules (grain sizes less than 4 mm), thus it has the appearance of being fine-grained overall. In gravel-bed rivers, these finer sizes would be entrained and transported quite easily were it not for the rate-limiting effects introduced by the armor layer; coarse clasts within the armor layer hinder the movement of finer grains, thus limiting their mobility in relation to the available shear stress.

Transport measurements in gravel-bed rivers indicate that clasts within the armor layer typically begin moving at flows ranging from about one-half to two-thirds of the bankfull discharge (Mueller *et al.*, 2005). As discharge increases, more bed material is entrained, and there is an increase in both the flux and grain size of the bed load (Milhous, 1973; Jones and Seitz, 1980; Kuhnle and Willis, 1992; Andrews, 1994; Wathen *et al.*, 1995; Powell *et al.*, 2001; Ryan and Emmett, 2002; Clayton and Pitlick, 2007a). However, as illustrated in Figure 1, the grain size of the bed load increases rather slowly in comparison to the flux, thus for typical sediment-transporting flows the bed load is generally much finer than the surface (and perhaps finer than the substrate; Lisle, 1995). There is also some evidence indicating that under certain conditions the surface layer remains largely intact over the duration of a flood hydrograph (Andrews and Erman, 1986; Hassan *et al.*, 2006; Clayton and Pitlick, 2007b). As a consequence, the particles moving as bed load must slide or hop over and around the larger, mostly stationary particles forming the armor layer. In bed

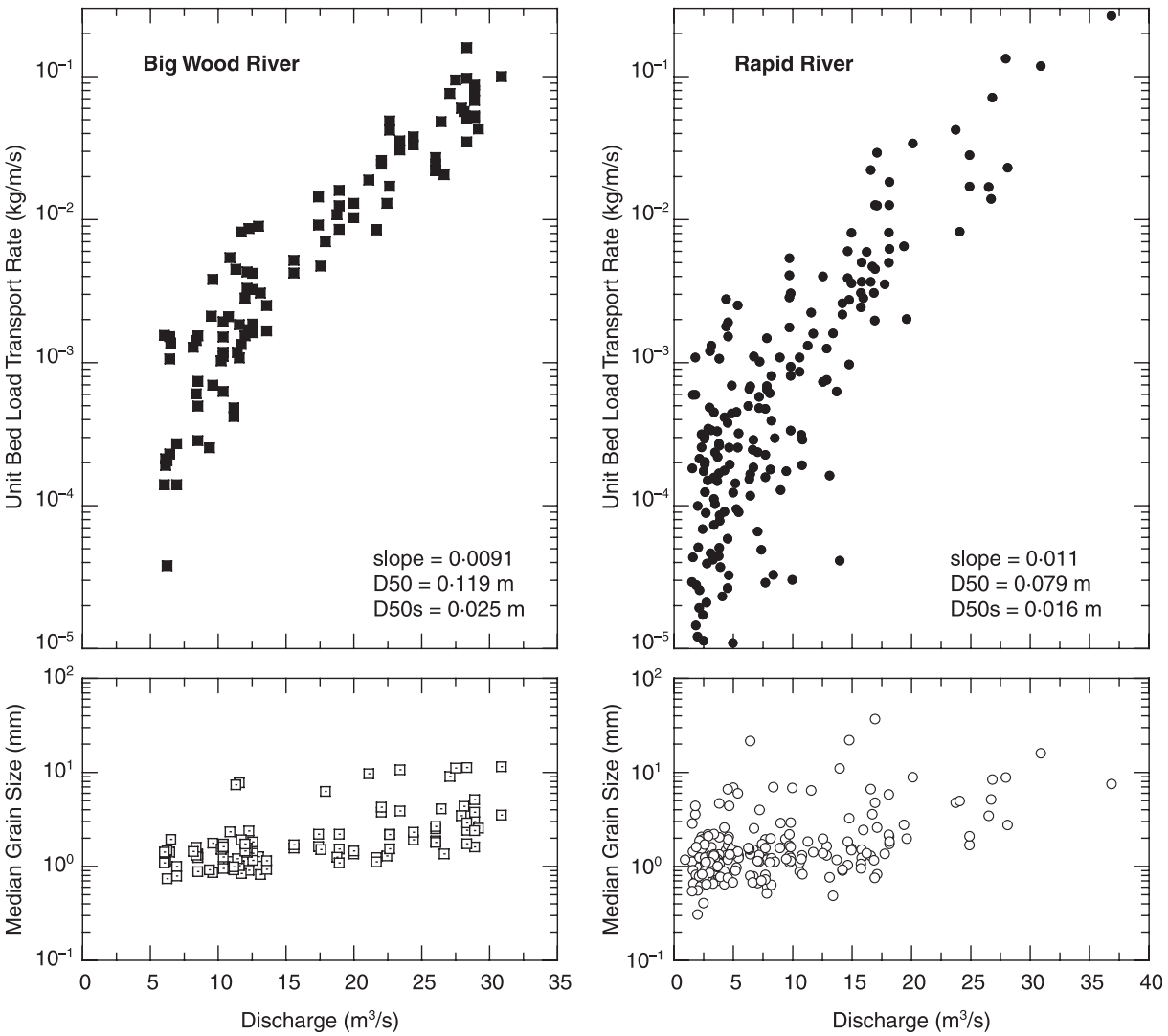

Figure 1. Changes in bed load transport rate and median grain size for two rivers in Idaho, USA.

load transport equations, differences in mobility of small and large particles are accounted for by a so-called hiding function, $f(D_i/D_{50})$, where D_i is an individual grain size and D_{50} is the median grain size. Let us assume for the moment that D_i and D_{50} are characteristic grain sizes of the bed load and bed surface, respectively, and that $D_i < D_{50}$, as noted above. Let us also assume that the substrate is the primary source of the bed load, thus D_i is equivalent to the substrate median grain size, D_{50s}. In a channel network, both D_{50} and D_{50s} should become finer downstream due to selective transport, deposition and/or abrasion. If the two sizes fine at the same rate, then the ratio of D_{50} to D_{50s} is constant, and the effects of hiding and exposure stay the same in a relative sense. Alternatively, if the two sizes fine at different rates, the hiding–exposure effects may offset changes in shear stress and limit (or enhance) the mobility of the bed load as it moves through the network. Both hypotheses are reasonable; however, conditions favoring one versus the other have not been explored, nor have the implications with respect to models of downstream fining or drainage basin evolution.

In this paper, we examine interactions between reach-scale flow properties and trends in surface and substrate grain sizes. We have amassed a large data set from field studies of gravel- and cobble-bed rivers in Colorado and Utah that allows us to examine relations between shear stress, armoring and bed load transport intensity over a broad range of scales. Additional data from studies conducted elsewhere in the USA are included to assess the applicability of our results. The implications of the results are then explored using a conceptual model that links flow properties to a set of

DOI: 10.1002/esp

relations governing transport thresholds and transport intensity. The model results suggest that the mass balance of bed load in a channel with decreasing slope is maintained by tradeoffs between the available shear stress relative to the threshold shear stress, and the grain size of the bed load relative to the grain size of the surface layer.

Study Area and Methods

Study Sites

The primary data set used for this analysis is developed from field measurements at 105 different locations on gravel-bed rivers in Colorado and Utah, USA. These data were collected as part of separate field studies completed from 1993 to 2005: the objectives of these studies were different; however, the methods used in collecting the data were consistent. The study sites are divided between those located on relatively small gravel-bed streams in subalpine basins in the southern Rocky Mountains, and two large gravel-bed rivers on the Colorado Plateau – the Gunnison River and the Colorado River. Site characteristics vary accordingly. The subalpine streams drain forested basins that are generally stable against erosion; annual bed load sediment yields in these basins are low (<5 t/km^2/yr) (Torizzo and Pitlick, 2004; Mueller and Pitlick, 2005). Drainage areas of these streams range from 3 to 300 km^2, average channel gradients range from 0·001 to 0·07 m/m and bankfull widths range from 3 to 24 m (Table I).

The study reaches on the Gunnison River and the Colorado River are located in western Colorado and eastern Utah. Vegetation in surrounding areas is sparse, and underlying rock types (interbedded shale and sandstone) are susceptible to surface erosion; annual sediment yields are 30–90 t/km^2/yr (Pitlick and Cress, 2002), of which about 5% is carried as bed load (Pitlick and Van Steeter, 1998). Drainage areas above the study reaches range from 14 500 to 62 400 km^2, slopes range from 0·0005 to 0·002 m/m, and bankfull widths range from 60 to 360 m (Table I). Additional details on site characteristics are discussed in the references listed in Table I, and a spreadsheet copy of the complete data set can be obtained by request from the first author.

Although the study sites are located within the same general geographic region, there are some important differences in site characteristics. The subalpine streams drain glaciated basins with relatively dense forest cover below elevations of ~3000 m. These basins are underlain by crystalline rock. The rivers on the Colorado Plateau flow through sparsely vegetated areas underlain by sedimentary rock; these rivers carry a mixture of locally derived sedimentary rock, plus crystalline rocks transported from the same high-elevation region as described above. The crystalline and sedimentary rocks likely differ in their resistance to abrasion. Bank vegetation is very different in the alpine and plateau settings, as is the percentage of the total load carried in suspension; these two characteristics likely influence bank strength, and thus channel geometry. In spite of these differences, it is fair to say that these streams and rivers are relatively stable in a hydrologic or geomorphic sense. The flow regime is dominated by an annual spring snowmelt that lasts several weeks, and events that trigger landslides or debris flows are uncommon.

A companion data set developed from separate studies of bed load transport in 30 other gravel-bed streams and rivers in the western USA is used for comparison with our observations. In addition to measurements of channel geometry and average gradient, the companion data set includes measurements of grain size for both the surface and substrate sediment. Twenty-three of these sites are located in mountainous areas of Idaho, thus they are similar in many senses to the subalpine streams in Colorado – they drain forested basins underlain by crystalline rocks, with the majority of the annual runoff produced by spring snowmelt (Mueller *et al.*, 2005). Drainage areas of these streams and

Table I. Range in study site characteristics

River basin	Number of sites	Drainage area (km^2)	Average slope (m/m)	Bankfull	
				Width (m)	Depth (m)
Colorado River[1]	12	18 000–62 400	0·0003–0·002	76–360	2·1–6·5
Gunnison River[2]	9	14 600–20 500	0·001–0·002	57–89	2·8–3·3
Halfmoon Creek[3]	27	3·0–64	0·006–0·07	2·5–12	0·2–0·6
Williams Fork[4]	18	14–300	0·004–0·04	4·4–24	0·4–0·9
Colorado,various[5]	12	30–230	0·001–0·04	4·5–21	0·5–0·9
Western USA, various[6]	30	15–240 800	0·0003–0·05	4·3–89	0·2–5·3

Data sources: [1] Pitlick *et al.*, 1999; [2] Pitlick and Cress, 2002; [3] Mueller and Pitlick, 2005; [4] C. Segura, unpublished data; [5] Torizzo and Pitlick, 2004; [6] Mueller *et al.*, 2005.

DOI: 10.1002/esp

rivers range from 15 to 5000 km^2, average gradients range from 0·0005 to 0·05 m/m and bankfull widths range from 4 to 89 m (Table I). Sediment yields of these streams and rivers are on the order of 10–30 t/km^2/yr (Kirchner *et al.*, 2001). Additional information for these sites is given in a series of on-line reports available through the US Forest Service (King *et al.*, 2004). The remaining seven sites are scattered throughout the western USA in areas of mixed bedrock lithology and forest cover (Mueller *et al.*, 2005). Drainage areas of these streams range from 14 to 241 000 km^2, average gradients range from 0·0003 to 0·02 m/m and bankfull widths range from 5 to 190 m. We were not involved in data collection at these sites; however, the descriptions of field methods provided in the published reports and papers indicate that the measurement and sampling procedures were very similar to ours, as described below.

Field Data

Measurements of the bankfull channel geometry, average channel gradient and bed material grain sizes were made in each reach using consistent surveying and sampling methods. Channel characteristics, including bankfull channel width, B, bankfull channel depth, H, and reach-average slope, S, were measured using a combination of surveying instruments. In reaches that could be waded, cross sections and average gradients were measured with an engineering level and a fiberglass rod; slopes were measured over distances of 10–20 times the bankfull channel width. In reaches that could not be waded, cross sections were measured with a total station and a motorized rubber raft outfitted with a depth sounder. Average gradients in these reaches were measured with a mapping grade global positioning system (GPS). Readings of the water surface elevation were taken with the GPS at 0·8 km intervals, and subsequently corrected using differential post-processing techniques. The vertical error of the individual GPS measurements on the larger rivers (Colorado R. and Gunnison R.) was typically ~0·5 m; this is high in comparison with leveling measurements taken in the smaller streams, but low in relation to the total drop in water surface elevation through specific study reaches.

Samples of the surface sediment were taken in wadeable portions of the channel, or on exposed gravel bars within or very near the study reach. The surface layer was sampled using the Wolman method, with a minimum of 100 particles sampled at random across the bed or bar surface. Particle sizes were measured with a metal template (gravelometer) with 1/2-psi openings ($\psi = \log_2 D$, where D is the grain size in mm). Bulk samples of the substrate were taken on subaerially exposed gravel bars by removing the surface layer clasts, and extracting 50–300 kg of sediment from the bed, depending on the weight of the largest individual grain. In all but a few cases the largest grain represented no more than 5% of the bulk sample weight, and often much less. Our samples fall short of the conservative criteria proposed by Church *et al.* (1987), but within the negligible-bias, good-precision criteria of Ferguson and Paola (1997). The coarse fraction (>32 mm) of the substrate was sieved in the field, and the fine fraction (<32 mm) was sieved in the laboratory, both at 1/2-psi intervals.

In reviewing methods for sediment sampling and analysis, Church *et al.* (1987) suggested that comparisons between surface and substrate grain size distributions (GSDs) should be based on the same size range (truncated), if representative samples of one or the other cannot be taken. If the surface includes a significant proportion of fines, for example, then a grid-based sample is not likely to be representative of the surface GSD, nor comparable to a bulk sample of the substrate; therefore, the two GSDs should be adjusted to a common range of sizes. Likewise, a surface sample of an immobile armor formed from winnowing of fines, as might occur in a sediment-starved reach downstream of a dam, represents a truncated version of the bulk bed material, thus the fines should be excluded from comparing surface and substrate GSDs. A third case, which lies somewhere in between these two, is a mobile armor layer formed as a result of equilibrium transport. In this case, the concentration of coarse particles on the bed surface is a fundamental part of the process, thus the rationale for truncating the GSD is not as clear as it is in the other cases. Conditions at our sites are consistent with the model of equilibrium transport; therefore, we did not see a clear reason for truncating the GSDs of our samples. Particles finer than ~8 mm are generally not abundant in our samples. Furthermore, in taking these samples, we often observed that the coarsest clasts on the bed were loose, thus we would not characterize the surface as a static armor. Most of the surface-layer particles are capable of being transported by flows that occur at least a few days a year (Mueller and Pitlick, 2005; Torizzo and Pitlick, 2004; Pitlick and Cress, 2002). The proportion of surface-layer particles moving at high flows is probably never very large; however, we assume that eventually most sizes do move, allowing the bed load and substrate to exchange with each other.

The measurements of channel geometry and grain size were used with uniform flow relations to estimate relevant hydraulic variables, including the bankfull discharge,

$$Q = BHU \tag{1a}$$

bankfull velocity,

DOI: 10.1002/esp

$$U = \left(\frac{8gRS}{f}\right)^{1/2} \tag{1b}$$

friction factor,

$$\frac{1}{\sqrt{f}} = 2{\cdot}26 \log\left(\frac{R}{D_{84}}\right) + 1{\cdot}00 \tag{1c}$$

bankfull shear stress,

$$\tau = \rho g R S \tag{1d}$$

and bankfull dimensionless shear stress,

$$\tau^* = \frac{\tau}{(\rho_s - \rho)\, g\, D_{50}} \tag{1e}$$

In the above equations, R is the bankfull hydraulic radius, g is the gravitational acceleration, D_{84} and D_{50} are the 84th and 50th percentiles of the bed-surface grain size distribution, respectively, ρ_s is the density of sediment (2650 kg/m^3) and ρ is the density of water (1000 kg/m^3). The Gunnison River and Colorado River both have high width to depth ratios, thus H was used in place of R at sites on these rivers.

Field Observations

Particle-size distributions for each of the surface and substrate sediment samples are shown in Figure 2. This plot reveals the fundamental difference between surface and substrate sediment: the substrate contains a much higher

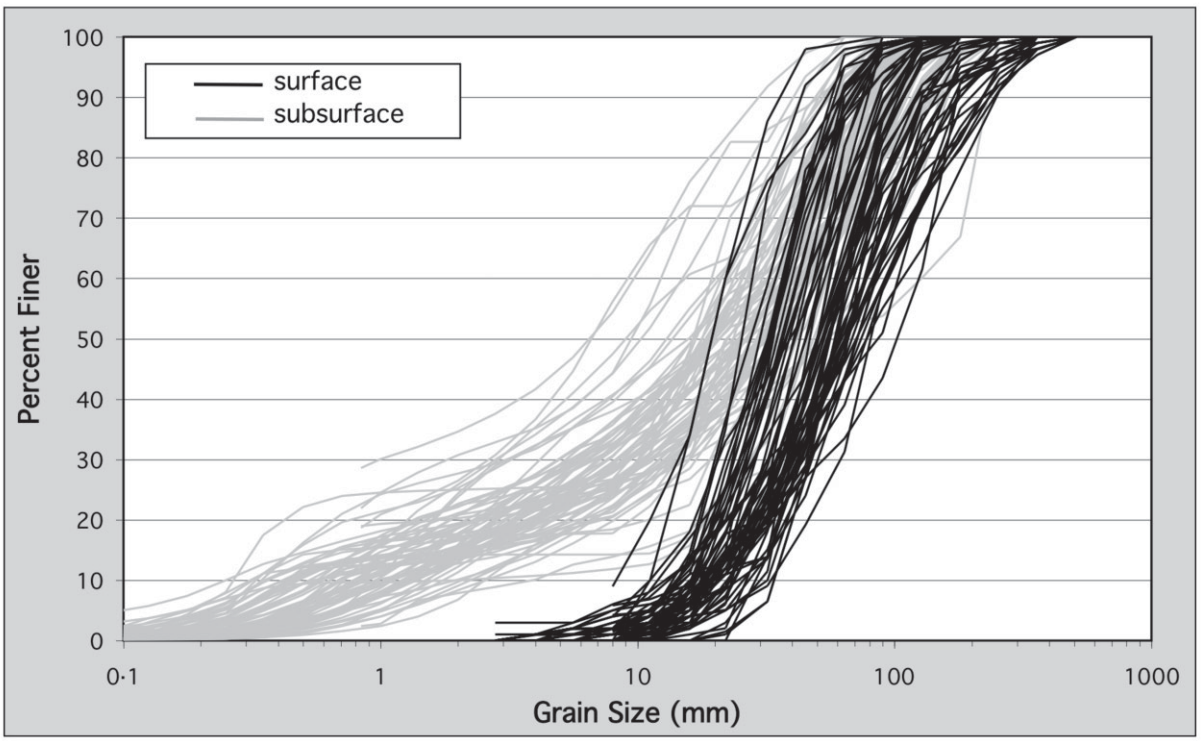

Figure 2. Grain size distributions of surface and substrate sediment measured at various sites throughout the southern Rocky Mountains and Colorado Plateau.

DOI: 10.1002/esp

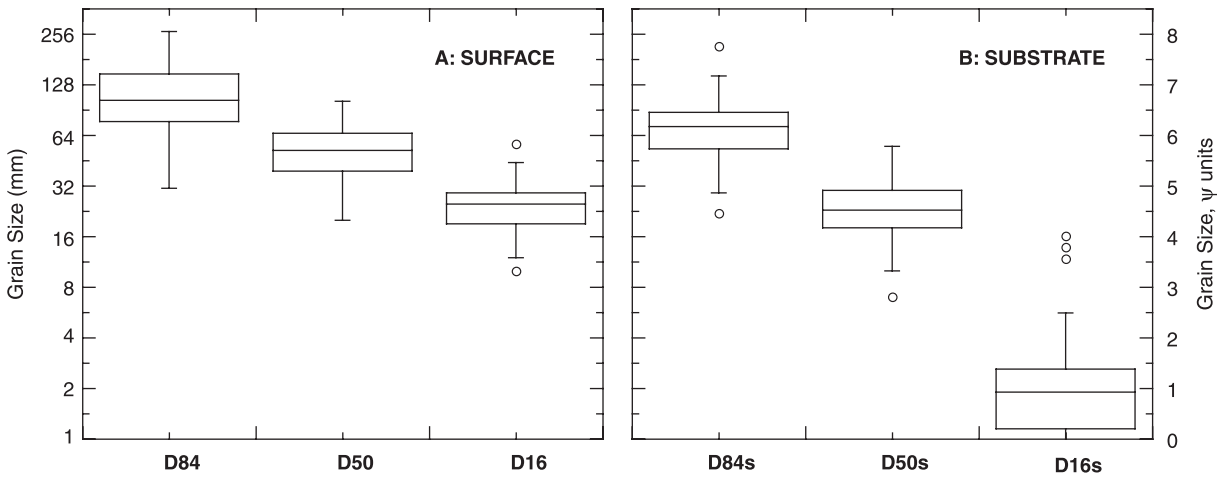

Figure 3. Box plots indicating the range in individual grain size parameters for (a) surface and (b) substrate grain size distributions.

percentage of sand and fine gravel ($D < 8$ mm) than does the surface. Our data indicate that 20–40% of the substrate is comprised of sand and fine gravel, whereas these sizes are generally absent from the surface. The contrast between surface and substrate sediment clearly becomes less distinct as grain size increases, and there is significant overlap in the coarser size fractions. The coarsest grain sizes seen on the bed surface are commonly present in the substrate, although in smaller numbers.

The general characteristics of the grain size distributions are summarized in Figure 3 by a series of box plots showing the range in grain size percentiles of surface and substrate samples. The upper panel (Figure 3(a)) shows that there is a wide range in the coarse- and intermediate-size fractions of the surface-layer samples. The D_{84} of the bed surface varies from a low of 31 mm to a high of 264 mm (more than a 3 ψ range), with 50% of the values falling in the 1 ψ interval from 64 to 128 mm. The D_{50} of the bed surface varies from a high of 102 mm to a low of 20 mm (a range of 2·4 ψ), with 60% of the sample values falling in the 1 ψ interval from 32 to 64 mm. The range in D_{16} is similar. The difference between median values of D_{84} and D_{16} is about 2 ψ, reflecting the fact that the bed surface is generally well sorted.

The overall range in substrate grain sizes is clearly greater than surface, largely because of the abundance of fine gravel and sand (Figure 3(b)); the difference between the median values of D_{84} and D_{16} in the substrate is greater than 5 ψ. However, the variation within intermediate- and coarse-size fractions of the substrate is not as large as it is in the surface: the D_{84} of the substrate ranges from 22 to 220 mm (Figure 3(b)), with 77% of the sample values falling in the 1 ψ interval from 45 to 90 mm. The D_{50} of the substrate ranges from 7 to 55 mm (Figure 3(b)), with 80% of the sample values falling in the 1 ψ interval from 16 to 32 mm.

The companion data sets for other streams in the western USA did not always include a listing of the full grain size distribution of the bed surface or the substrate, thus we cannot make the same comparisons between individual grain size percentiles as above. However, the median grain sizes of the surface and substrate were reported in each study, thus we can compare these values against the values obtained in the present study. Figure 4 shows separate histograms plotting the frequency distribution of surface and substrate D_{50} for the two data sets, labeled Colorado and Idaho, respectively. This figure reinforces the point made above that the range in substrate D_{50} is much less than the range in surface D_{50}, and this appears to be true of both data sets. What is perhaps more interesting, however, is the overlap in the measured values of substrate D_{50}; both frequency distributions exhibit a prominent mode centered around 20 mm, and the mean of each distribution is about the same, 24 and 25 mm, respectively. Although separated geographically, the sediment stored in the bed of these stream systems is evidently similar, and consistently finer than the sediment that forms the armor layer.

A large part of the variation in armor layer grain sizes can be explained by variations in channel gradient and flow depth, which together determine the magnitude of the local boundary shear stress, τ. Figure 5 plots the relation between bankfull τ and four separate percentiles of the surface and substrate grain size distributions. The data in the top panel (Figure 5(a)) show that the bed-surface grain sizes are strongly correlated to the bankfull shear stress. The individual points tend to scatter uniformly about these lines, and both relations are statistically significant ($p < 0{\cdot}001$, Table II). In addition, the standard errors of the regression coefficients, SE_a and SE_b, are both small in relation to the

DOI: 10.1002/esp

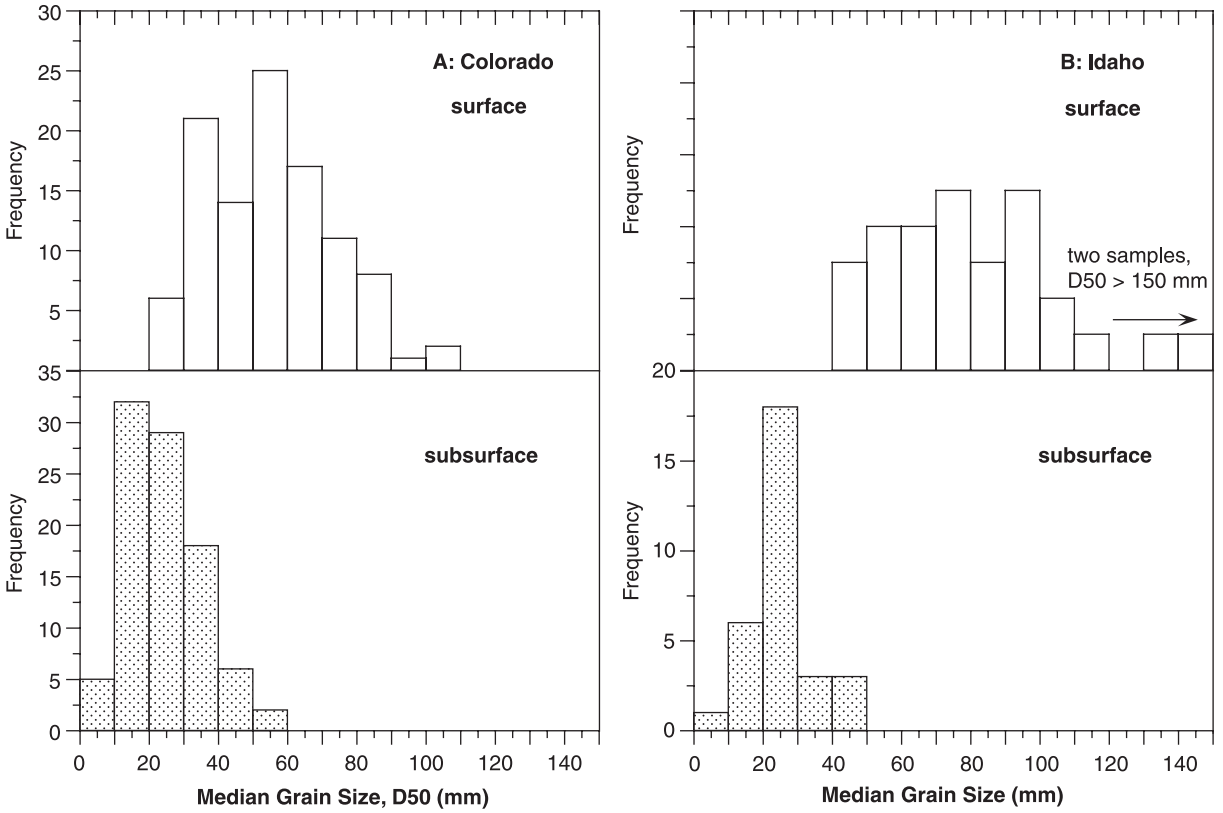

Figure 4. Frequency distributions of surface and substrate median grain sizes for study sites in (a) Colorado and (b) Idaho.

Table II. Summary statistics for regression relations shown in Figures 5–8; *a* and *b* are parameters of the linear relation, log $Y = \log a + b \log X$; values shown in parentheses are standard errors of the regression coefficients, SE_a and SE_b; SE_r is the standard error of the regression; r^2 is the coefficient of determination and *p* is the significance probability

	a	*b*	SE_r	r^2	*p*
Figure 5					
D_{84}	−1·78	0·46	0·13	0·55	<0·001
	(0·072)	(0·041)			
D_{50}	−1·84	0·32	0·12	0·43	<0·001
	(0·063)	(0·036)			
D_{84s}	−1·55	0·23	0·15	0·19	<0·001
	(0·087)	(0·050)			
D_{50s}	−1·73	0·04	0·20	<0·01	0·56
	(0·118)	(0·067)			
Figure 6					
D_{50}	−1·47	0·22	0·097	0·13	0·05
	(0·190)	(0·105)			
D_{50s}	−1·57	−0·02	0·087	<0·01	0·78
	(0·157)	(0·087)			
Figure 7					
D_m/D_{50}	0·17	−0·31	0·151	0·30	<0·001
	(0·073)	(0·041)			
Figure 8					
τ^*_{r50s}	0·093	0·41	0·223	0·55	<0·001
	(0·078)	(0·034)			
τ^*_{r50}	−0·44	0·46	0·172	0·64	<0·001
	(0·114)	(0·052)			

DOI: 10.1002/esp

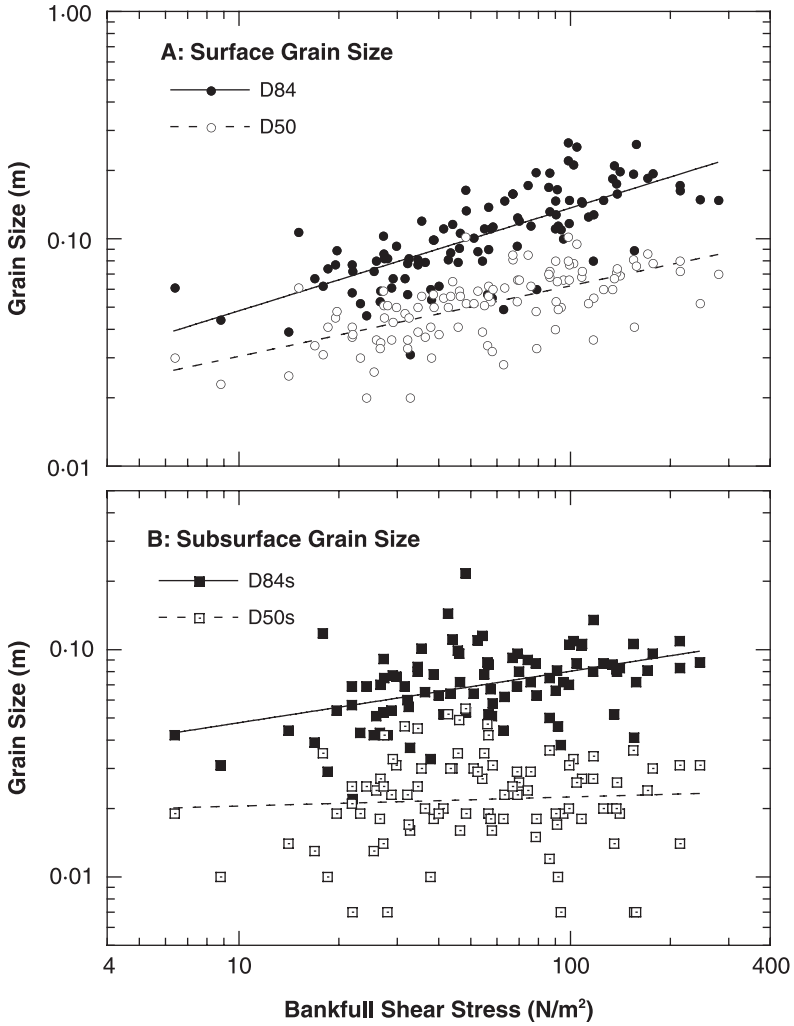

Figure 5. Relation between bankfull shear stress and four separate percentiles of (a) surface and (b) substrate grain size distributions of streams in Colorado.

coefficients themselves (Table II). The main feature of Figure 5(a) is the difference in the slopes of the relations for D_{84} and D_{50}. This difference in slopes suggests that the coarser fractions of the bed surface grain size distribution are more strongly associated with the shear stress than intermediate size fractions; thus, as the stress increases, the difference between D_{84} and D_{50} also increases (sorting decreases). The other point to note here is that the coefficient b in the relation for D_{50} is much less than 1·0, which would be the case if the grain size increased in proportion to the shear stress (i.e. if the bankfull τ^* was constant; see Parker, 1979; Dade and Friend, 1998; Pitlick and Cress, 2002; Parker *et al.*, 2007). This discrepancy is due primarily to the increase in fluid drag caused by large roughness elements (boulders and cluster bedforms), which alter the vertical distribution of velocity and shear stress, particularly in steep channels. Under these conditions, a large proportion of the total stress is expended as form drag, and the bed surface tends to be finer than expected for a given depth and slope.

The lower panel in Figure 5 shows similar relations for the substrate parameters, D_{84s} and D_{50s}. A clear trend is evident in the relation between D_{84s} and bankfull τ, and the statistical measures of fit are similar to the surface-based relations discussed above (Table II). In contrast, the relation between D_{50s} and bankfull τ is not statistically significant ($p = 0{\cdot}56$, Table II), and the standard errors of the regression coefficients are both relatively large. The results in Figure 5(b) indicate that there is essentially no correlation between the median grain size of the substrate and the reach-average shear stress.

DOI: 10.1002/esp

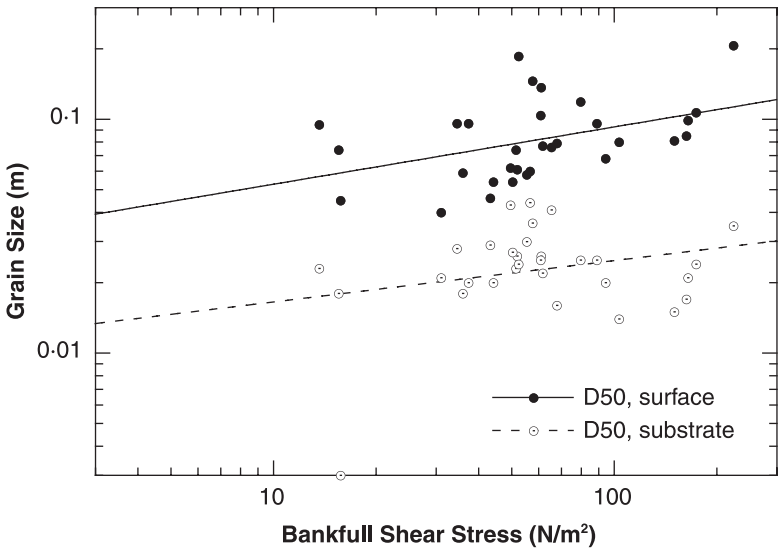

Figure 6. Relation between bankfull shear stress and surface and substrate median grain sizes of streams in Idaho.

Figure 6 shows similar relations for the companion (Idaho) data set, plotting only the trends for the surface and substrate D_{50}. In this case, the relation between bankfull τ and surface D_{50} is not especially strong ($r^2 = 0{\cdot}13$; Table II); nonetheless, the relation is significant at the 0·05 level. Similar to the Colorado data set, the correlation between the substrate D_{50} and the bankfull τ is poor ($r^2 < 0{\cdot}01$, Table II) and the relation is not statistically significant ($p = 0{\cdot}78$, Table II).

The results presented above suggest that surface and substrate grain sizes follow separate trends over the range of observed shear stresses. It follows that the ratio of substrate D_{50} to surface D_{50} should vary inversely with the bankfull τ. This appears to be the case, as shown in Figure 7. A least squares fit of these data gives the relation

$$\frac{D_{50s}}{D_{50}} = 1{\cdot}48\,\tau^{-0{\cdot}31} \tag{2}$$

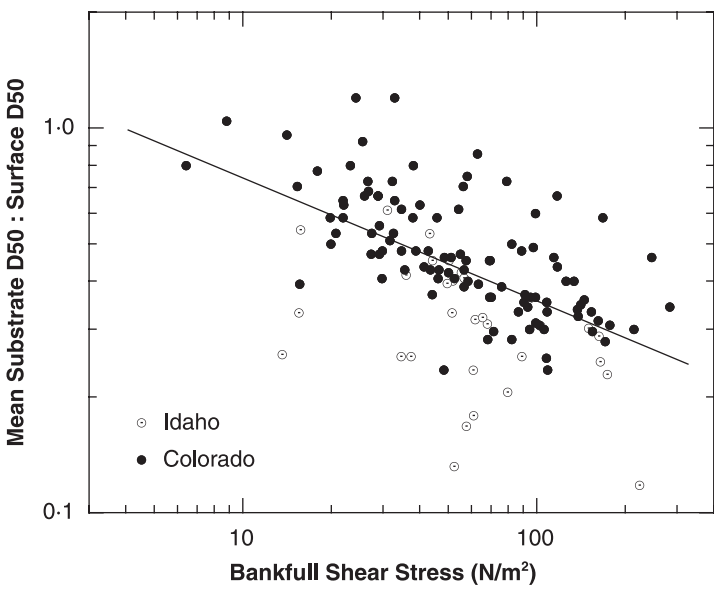

Figure 7. Relation between bankfull shear stress and the ratio of substrate D_{50} to surface D_{50} for all study sites.

DOI: 10.1002/esp

The scatter in these data spans nearly one log cycle; however, the relation given by Equation (2) is statistically significant ($p < 0{\cdot}001$, Table II), and the coefficients a and b both have relatively low standard errors. The trend line indicates that in low gradient reaches, with bankfull shear stresses on the order of 10 N/m^2, the expected value of D_{50s}/D_{50} is approximately 0·8, meaning the surface D_{50} is only slightly larger than the substrate D_{50}. In steep headwater reaches, with shear stresses on the order of 100 N/m^2, the expected value of D_{50s}/D_{50} is approximately 0·3, thus the surface D_{50} is about three times as large as the substrate D_{50s}. In the section that follows we set up a simple model to examine potential implications of this result by contrasting downstream trends in transport intensity under the assumption that (a) the surface and substrate fine at the same rate, giving a constant ratio of D_{50s}/D_{50}, versus (b) the results presented above suggesting that the surface and substrate fine at different rates, giving a ratio of D_{50s}/D_{50} that varies inversely with shear stress.

Potential Implications

The broader implications of the field data are explored below using a conceptual model that couples relations for flow, channel geometry and grain size to calculate the total bed load flux through a hypothetical drainage basin. The model is based on the results presented above showing that the median grain size of the substrate, D_{50s}, is relatively consistent from one place to another, whereas the D_{50} of the armor layer varies systematically with the local shear stress. The effects of drainage basin scale are represented in the model by downstream trends in slope and channel geometry, estimated by coupling relations for hydraulic geometry, continuity and flow resistance. Transport rates are calculated for bankfull flow under the assumption that the bed load moving through individual reaches has the same grain size distribution as the substrate within that reach. This assumption forms the basis of several transport models (Parker *et al.*, 1982; Dietrich *et al.*, 1989) and implies that the substrate is the primary local source of bed load. It also allows us to take advantage of the results presented above to explore how differences in the ratio of D_{50s} to D_{50} affect the mobility and mass flux of bed load as it moves through a channel network.

Model Formulation

The characteristics of the hypothetical channel are modeled after cobble- and gravel-bed streams in the southern Rocky Mountains, USA. The bankfull discharge, Q, is specified at individual points along the channel using a regional hydrologic relation presented by Mueller and Pitlick (2005):

$$Q = 0{\cdot}30A^{0{\cdot}75} \tag{3}$$

where A is the drainage area, in square kilometers. The coefficient in this relation is specific to the region; however, the exponent is similar to values obtained in other studies (e.g. Emmett, 1975; Cinotto, 2003). A is allowed to vary from 4 to 5000 km^2. The range in A is arbitrary, but, when coupled with a relation between length and drainage area, $L = 1{\cdot}5A^{0{\cdot}6}$, this gives a channel that is ~160 km long, which is representative of moderate-sized gravel-bed rivers in this region. The reach-average slope, S, is assumed to vary inversely with the bankfull discharge:

$$S = 0{\cdot}04Q^{-0{\cdot}60} \tag{4}$$

where the coefficient 0·04 and exponent –0·60 are chosen to give slopes ranging from 0·04 to 0·002 m/m for the range in A and Q. The bankfull R and bankfull B are specified by downstream hydraulic geometry relations:

$$R = 0{\cdot}25Q^{0{\cdot}30} \tag{5a}$$

$$B = 3{\cdot}8Q^{0{\cdot}50} \tag{5b}$$

where the coefficients and exponents are chosen to give values of R ranging from 0·2 to 1·2 m, and values of B ranging from 4 to 50 m. The coefficients and exponents in these equations are based on results from previous work, giving values of S, R and B consistent with free-flowing gravel-bed rivers in the southern Rocky Mountains (Andrews, 1984; Torizzo and Pitlick, 2004).

Bed load transport rates are calculated at individual points along the channel using the Parker (1979) transport function. This function is used because it is straightforward to implement, and the individual parameters are formulated in ways that allow us to make use of the results presented herein. We examined the effects of using other transport functions, such as Parker (1990), and Wilcock and Crowe (2003), and found that the results were qualitatively very similar, regardless of the function used. Parker's transport function can be written as

DOI: 10.1002/esp

$$W^* = 11{\cdot}2\left(1 - \frac{0{\cdot}853}{\phi}\right)^{4{\cdot}5} \tag{6}$$

where W^* is a dimensionless transport parameter and ϕ is a dimensionless transport stage. These two terms are defined as follows:

$$W^* = \frac{(s-1)gq_b}{\rho_s(\tau/\rho)^{1{\cdot}5}} \tag{7}$$

where s is the specific gravity of sediment, q_b is the mass transport rate per unit width and

$$\phi = \frac{\tau^*}{\tau_r^*} \tag{8}$$

where τ^* is the dimensionless shear stress (1e), and τ_r^* is the reference dimensionless shear stress.

The numerator in (8) is estimated for bankfull flow conditions by combining the Colorado–Idaho data sets to form an empirical relation between bankfull τ^* and reach-average gradient. This relation, shown in Figure 8(a), is similar to one presented by Mueller *et al.* (2005), which accounts for increases in boundary shear stress in steep, shallow flows

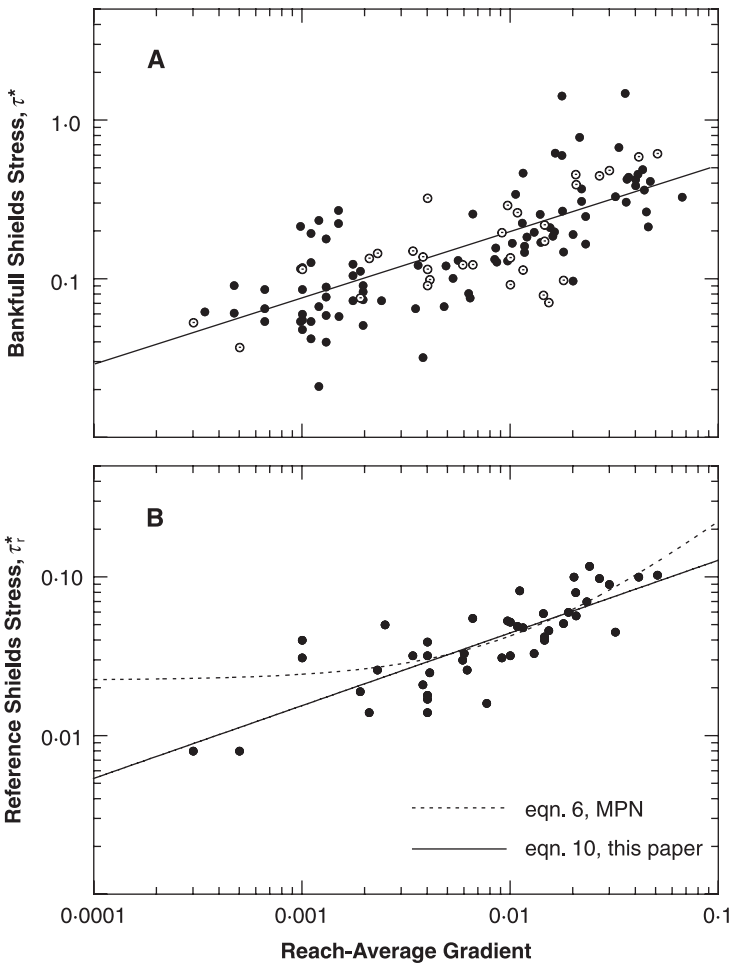

Figure 8. (a) Relation between bankfull Shields stress, τ^*, and reach-average gradient, S, for the study sites used in this analysis. Values of τ^*_{50s} were formulated using field-based estimates of bankfull shear stress and the substrate median grain size, D_{50s}. (b) Relation between reference Shields stress, τ_r^*, and reach-average gradient, S; the dashed line, labeled MPN, is Equation (6) in Mueller *et al.* (2005), while the solid line is a power-law fit to the same data.

DOI: 10.1002/esp

where boulders and cobbles dominate flow resistance. The individual values of τ^* shown in Figure 8(a) are formulated using the bankfull τ and the substrate D_{50}. A least-squares fit of these data, excluding the two values of $\tau^*_{50s} > 1{\cdot}0$, gives

$$\tau^*_{50s} = 1{\cdot}23S^{0{\cdot}41} \tag{9}$$

where the subscript s refers to the substrate D_{50}, and S is the reach-average gradient. While there is appreciable scatter in these data, and SE_a is of the same order as a (Table II), SE_b is relatively low, and the relation is statistically significant ($p < 0{\cdot}001$, Table II).

The denominator in (8) is estimated by coupling a relation presented by Mueller *et al.* (2005) with a hiding function. Mueller *et al.* (2005) compiled measurements of flow and bed load transport in 45 gravel-bed streams and rivers in western North America. For each data set, they plotted a relation between W^* and τ^*, and estimated the reference dimensionless shear stress, τ^*_{r50}, for the median grain size of the bed surface. They found that the fluid-drag effects of large roughness elements carried over into the individual transport relations, resulting in systematic shifts in τ^*_{r50} with increasing gradient. The data set used in that analysis is shown in Figure 8(b), along with the linear relation presented in the original paper, $\tau^*_{r50} = 0{\cdot}021 + 2{\cdot}18S$. For the purposes of this analysis and for consistency, we fit the same data with a power law,

$$\tau^*_{r50} = 0{\cdot}36S^{0{\cdot}46} \tag{10}$$

This relation is statistically significant ($p < 0{\cdot}001$), and the two regression coefficients both have relatively low standard error (Table II). It is evident from Figure 8(b) that the difference between linear and power-law fits is small over the range of model-specified slopes, 0·002–0·04. We opted to use (10) in these computations only because all of the equations presented previously are written as power laws.

Finally, we used the results from (10) with a hiding function to estimate the reference dimensionless stress for the substrate D_{50},

$$\frac{\tau^*_{r50s}}{\tau^*_{r50}} = \left(\frac{D_{50s}}{D_{50}}\right)^{-\gamma} \tag{11}$$

where the exponent γ reflects size-dependent differences in entrainment and transport. For this exercise we assumed $\gamma = 0{\cdot}9$, implying entrainment is slightly size selective. Lower or higher values of γ affect the specific values of τ^*_{r50s} and ϕ, but not the overall trends.

In setting up this problem we have assumed that the substrate is the primary local source of the bed load, hence D_{50s} represents a characteristic grain size of the bed load. The particles forming the surface layer are another potential source of bed load; however, we assume that, over the duration of a flood, these particles move infrequently, and as a result they act primarily as an irregular, nearly static surface over which the bed load must move. Bed load particles that stop moving become part of the surface layer, if only for an instant. Continued movement of those particles depends on local fluid forces, as well as their size in relation to neighboring particles, thus the assumed relation between D_{50s} and D_{50} becomes a key part of the transport problem when the substrate is considered as the primary source of bed load.

Transport rates are calculated for two scenarios: In the first scenario, we assume that the surface and substrate particles fine at the same rate, such that the ratio of D_{50s} to D_{50} is constant; an arbitrary value of $D_{50s}/D_{50} = 0{\cdot}5$ is chosen for this case. In the second scenario, we assume that the surface and substrate fine at different rates, such that the ratio of D_{50s} to D_{50} varies according to (2). The difference in these two scenarios directly affects the calculation of τ^*_{r50s} in (11). If the bed is strongly armored, the ratio of D_{50s} to D_{50} will be small, which will lead to a relatively high value of τ^*_{r50s} for a given τ^*_{r50}; this in turn leads to low values of ϕ and W^* for a given shear stress. Conversely, if the bed is only slightly armored ($D_{50s} \rightarrow D_{50}$), then the ratio of D_{50s} to D_{50} will be closer to 1·0, and the reference Shields stress for the substrate D_{50} will approach that of the surface D_{50} ($\tau^*_{r50s} \rightarrow \tau^*_{r50}$); such is the case in the absence of armoring.

Model Results

The assumed functional relations given by Equations (3)–(5) are plotted in Figure 9, with distance downstream used as a common scale. A finite distance of 160 km is used in place of a dimensionless distance to aid in visualizing trends at field scales. The relations used to specify discharge, slope, width and depth share the common feature of all being

DOI: 10.1002/esp

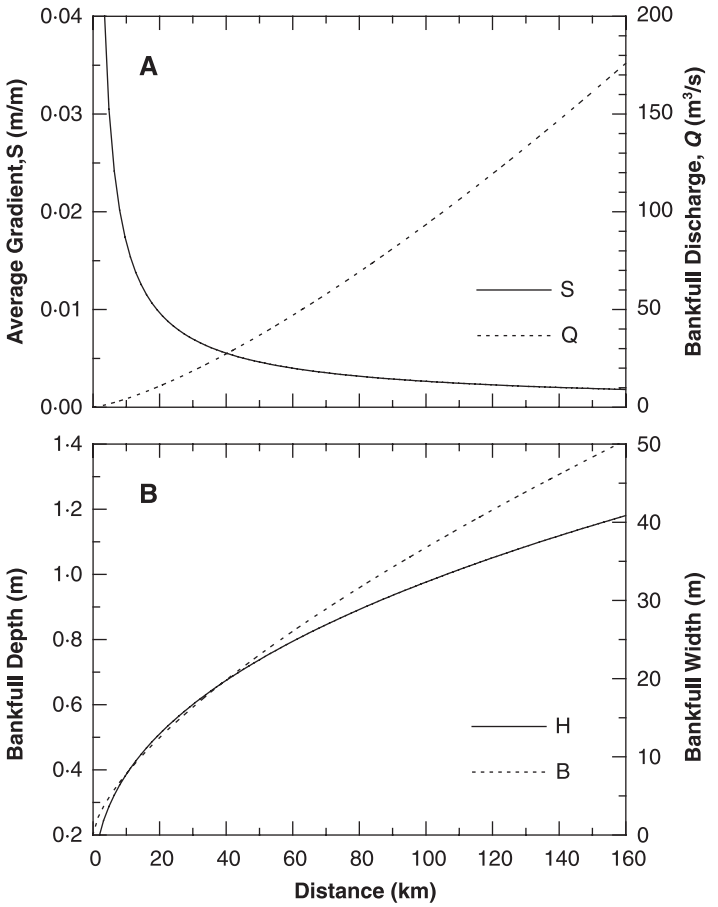

Figure 9. Downstream relations for average channel gradient, bankfull discharge, bankfull width and bankfull depth, defined by Equations (3)–(5).

nonlinear, thus considerable change takes place in the first 40 km of the model channel. Within this distance the slope decreases by almost an order of magnitude, while the bankfull width and depth increase by a factor of three. Although the range in values is determined by equations with somewhat arbitrary coefficients, these trends are representative of natural channels in regions with high relief.

As the distance increases, interactions among the individual variables become more complex, and this has a strong effect on calculated transport rates. The assumed relations for depth and slope lead to a rapid decrease in shear stress, from ~100 N/m^2 in the headwater reaches to ~20 N/m^2 in the distal reaches. The changes in stress affect the bed load transport parameters differently depending on the assumed relation between D_{50s} and D_{50}. Figure 10 shows separate trends in the reference Shields stress, τ^*_{r50s}, calculated from (11) under the assumptions stated previously: (a) the ratio of D_{50s} to D_{50} varies according to (2) and (b) the ratio of D_{50s} to D_{50} is constant. In both cases, the estimated τ^*_{r50s} decreases from values greater than 0·15 in the headwaters to values of less than 0·04 in downstream reaches. The general form of the two curves is governed by Equation (10), which is meant to capture the effect of form drag in steep channels. While the difference between the two curves does not appear to be large over the model domain, the crossover between headwater and downstream reaches has a strong influence on the mobility of substrate grain sizes. In the headwater reaches, estimated values of τ^*_{r50s} are higher in the channel where the ratio of D_{50s} to D_{50} is assumed to vary (solid line) than they are in the channel where the ratio of D_{50s} to D_{50} is assumed to be constant (dashed line). This difference reflects the operation of the hiding function (11), which can amplify or dampen variations in τ^*_{r50}, depending on the assumed relation between surface and substrate D_{50}. As noted above, if the bed is strongly armored, the ratio of D_{50s} to D_{50} will be low, and the value of τ^*_{r50s} computed from (11) will be relatively high for a given τ^*_{r50}. In this case particles supplied from the bed are much finer than the surface layer and they are more effectively hidden from the flow than coarser grains. As the difference between surface and substrate grain sizes narrows, the ratio of D_{50s}

DOI: 10.1002/esp

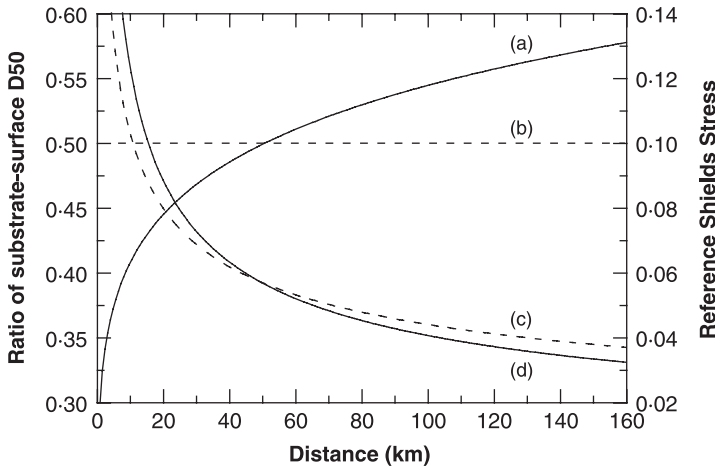

Figure 10. Downstream trends in bed-load transport modeling parameters; (a) shows the ratio of substrate to surface D_{50} given by Equation (2); (b) shows a constant value of the ratio, assuming the D_{50} of the substrate is half that of the surface; (c) and (d) show differences in the reference Shields stress for the substrate, τ^*_{r50s}, for conditions given by (b) and (a), respectively.

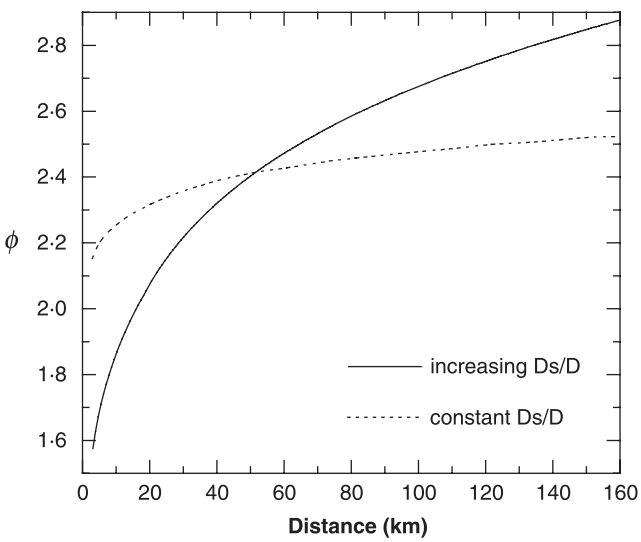

Figure 11. Downstream trends in bed-load transport intensity, ϕ, for hypothetical channels in which the bed becomes progressively less armored downstream (D_s/D increasing) and one in which there is no change in the relative degree of armoring (D_s/D constant).

to D_{50} increases, and the difference between τ^*_{r50s} and τ^*_{r50} gets smaller. The crossover that occurs at 55 km is the point where the armoring ratio is 0·5 in both cases. Below this point, the differences in armoring reverse, and the substrate grain sizes become increasingly more mobile downstream as the surface layer becomes finer.

Figure 11 shows that the differences in armoring have a potentially strong effect on the bed load transport stage, ϕ. In both scenarios, ϕ increases rapidly at first and more slowly thereafter. The differences in bed load transport stage reflect the inverse relation between τ^*_{r50s} and D_{50s}/D_{50} noted above. Thus, if the headwater reaches are strongly armored (solid line) the ratio of bankfull τ^*_{r50s} to reference τ^*_{r50s} tends to be small, resulting in much lower values of ϕ for a given τ^*. If the headwater reaches are not strongly armored (dashed line), substrate sizes are more mobile, leading to higher values of ϕ. Similar but opposite reasoning can be used to explain why transport stages then reverse below a distance of 55 km.

The differences in transport stage associated with the strength of armoring carry over into the calculated bed load transport rates, as shown in Figure 12. In both scenarios, the total (width-integrated) bed load transport rate, Q_s, increases rapidly at first (Figure 12(a)). Initially the total bed load is higher in the channel, where D_{50s}/D_{50} is assumed to be constant, again because the median grain size of the bed load is more nearly like the surface. The curves of Q_s

DOI: 10.1002/esp

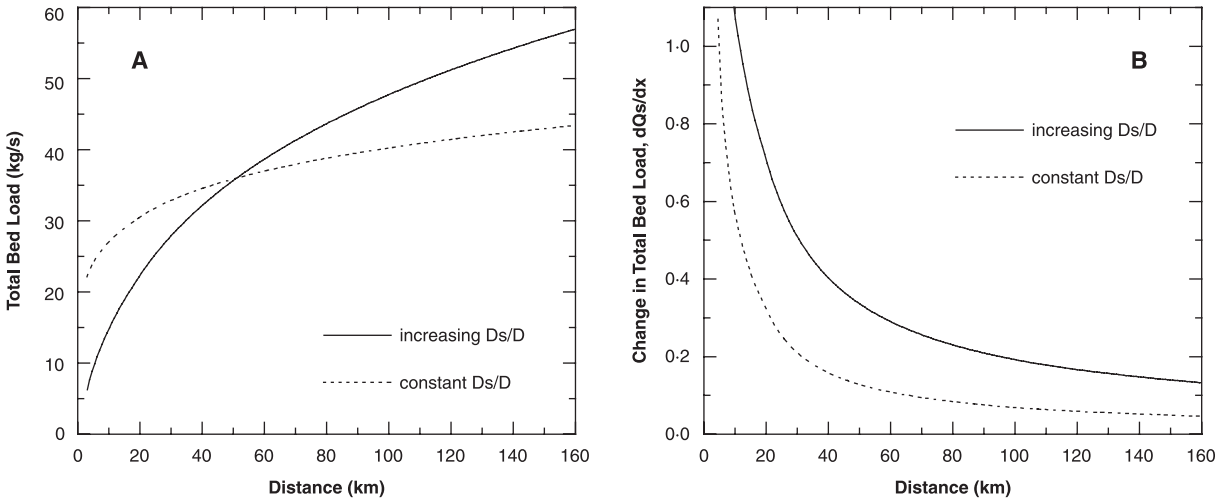

Figure 12. Downstream trends in (a) the instantaneous width-integrated bed load transport rate, Q_s, and (b) the change in total bed load transport rate, $\partial Q_s/\partial x$, for the two scenarios discussed in the preceding figures.

cross at the same point as noted above (55 km) and the channel with increasing D_{50s}/D_{50} then carries more bed load than the channel with a constant armoring ratio. At the downstream-most point, the difference in loads is 33%, thus the concentration of bed load is much higher in one channel than the other. If the load (or concentration) were forced to be the same, we would expect that the bed grain size or channel geometry would adjust to balance the differences in transport capacity.

The relations plotted in Figures 11 and 12 suggest that while there are some important differences in transport depending on the assumed role of armoring the curves for both ϕ and Q_s tend to flatten out with distance downstream. We can not say whether this behavior is typical of natural streams, but the trends imply that both model channels carry proportionally less bed load as drainage area increases. This may reflect 'real' processes, such as higher sediment supply in the headwaters, or the conversion of bed load to suspended load by abrasion, or it may simply reflect our assumption that transport rates at bankfull flow are representative of the full range of flows. It seems quite possible that downstream changes in transport intensity in natural channels could be offset by downstream changes in the frequency of bed load transport, as Mueller and Pitlick (2005) found in modeling transport through a small basin in Colorado. The importance of variations in transport frequency cannot be overstated; this remains an open question, requiring further research. Setting aside this point, the second panel in Figure 12 plots the change in total bed load with distance, $\partial Q_s/\partial x$, for the same two scenarios. These trends are of interest because they can be tied to channel morphology via the equation for sediment continuity, $\partial z/\partial t = \mathrm{M1}/(1\ \mathrm{M}\ \lambda)\partial Q_s/\partial x$, where z is the bed elevation and λ is the sediment porosity. The results in this plot suggest that, for the conditions specified, both channels would be erosional ($\partial Q_s/\partial x > 0$) over the full length of the basin, and the rate of erosion would diminish downstream, as might be expected. These conditions would not persist, of course, if the sediment supply changed or if the channel were otherwise allowed to evolve over time. Specifically, the slope would adjust according to the difference in transport rates, decreasing for all values of $\partial Q_s/\partial x > 0$. Furthermore, we would expect the composition of the bed material to change as sediment was exchanged between the bed load, the bed surface and the substrate. These processes will be explored in the future by developing a numerical model that tracks changes in individual grain sizes within the active layer as they exchange with the bed load, similar to the work of Hoey and Ferguson (1994, 1997).

Discussion

The field data and conceptual model presented here describe the sediment in gravel-bed rivers as consisting of two populations: the bed load and the substrate are one population, and the bed surface is another, separate, population. Enough information and data have been collected on other rivers to suggest that the first assumption (bed load = substrate) is more representative of some settings than others (see references listed in the introduction), thus our observations and results are applicable to a subset of gravel-bed rivers that are moderately active, yet stable in the near term. Differences among gravel-bed rivers are evident in several other examples. Field measurements similar to ours have

DOI: 10.1002/esp

been made in at least five other river systems: Vedder River and Fraser River, both in British Columbia, Canada (Martin and Church, 1995; Ferguson *et al.*, 2001; Church and Ham, 2004); the Waipaoa River in New Zealand (Gomez *et al.*, 2001); the Allt Dubhaig in Scotland (Ferguson *et al.*, 1996) and four streams in the Cascade and Olympic Mountain ranges in Washington, USA (Brummer and Montgomery, 2003). Among these studies, the first four report that the substrate D_{50} decreases systematically downstream, in clear contrast to the trends observed in our data. Furthermore, it appears that in three of these rivers (Fraser, Allt Dubhaig and Waipaoa) the substrate D_{50} scales consistently with the surface D_{50}; the ratio of substrate to surface D_{50} in Fraser River and Allt Dubhaig averages about 0·5, and in the Waipaoa River it averages about 0·25. Published descriptions of these rivers indicate they are aggrading, thus the consistent scaling of substrate–surface D_{50} likely reflects net deposition. The results presented by Brummer and Montgomery (2003) show that there is relatively little variation in the substrate D_{50} within streams in western Washington. The trends in surface D_{50} in the streams in Washington are more complex than other systems (downstream coarsening, followed by fining), apparently because of the influence of debris flows in low-order segments of the channel network. The streams studied by Brummer and Montgomery would not be described as stable, but they are not obviously aggradational, as is the case with the other river systems.

In aggradational systems the least mobile portions of the load are taken sequentially out of the system by deposition, leading to downstream fining of the bed material. In stable alluvial rivers the process of fining is harder to explain because the different grain sizes need to be transported at the same rate as they are supplied, whether the supply comes from the bed or nearby hillslopes. Ferguson *et al.* (1996) and Ferguson (2003) have argued that downstream fining is driven primarily by size-selective transport, which sets up a positive feedback between the bed texture and the bed load – similar to the arguments presented here – where fining enhances transport rates through reaches of rapidly decreasing shear stress. Gasparini *et al.* (1999, 2004) developed a basin-scale model suggesting that downstream fining arises naturally as a result of mutual adjustments in slope and bed surface texture to changes in water discharge and sediment supply. This model incorporates many of the same assumptions and/or observations discussed here, including the assumption that substrate texture is the same throughout the channel network, while the surface texture varies with the local gradient and shear stress. The model simulations suggest that channel slope and surface texture adjust dynamically to satisfy the requirement of equilibrium transport. Under steady state conditions the volume of sediment transported through the network must increase in proportion to the supply rate multiplied by the drainage area. They propose that as slope decreases downstream the bed surface becomes finer, thus lowering the threshold for transport and increasing transport efficiency, as suggested by Ferguson (2003). The results of these modeling studies are consistent with our interpretation of the field data, and suggest that differences in substrate and surface textures are of fundamental importance in modeling the long-term evolution of fluvial systems.

In interpreting the results of the conceptual transport model it is important to keep in mind that our calculations were restricted to a single flow (bankfull) with no specific accounting for the effects of differences in the frequency of bed load transport. Downstream differences in transport frequency are likely to have as much effect on bed load sediment yields as differences in transport intensity, and we encourage further research in this area. Evidence from a number of studies, including one of our own (Torizzo and Pitlick, 2004), indicates that the bankfull flow is often close to the flow that carries the most sediment (the effective discharge). However, it is not clear that the frequency of this single discharge varies systematically downstream, or with channel properties or other measures of basin scale. In developing sediment transport relations for a subset of the streams studied here, Torizzo and Pitlick (2004) and Whiting *et al.* (1999) found that there was no relation between the frequency of the effective discharge and drainage area. Emmett and Wolman (2001) examined differences in bed load transport relations among five sites in Idaho and Wyoming and found that the proportion of bed load carried by individual discharges shifted towards flows greater than bankfull as the slope of the bed load rating curve increased. Mueller and Pitlick (2005) made use of magnitude–frequency relations to calculate the annual bed load sediment yield at 27 individual points within a channel network, and found that, because of differences in transport thresholds, reaches with coarse sediment transported bed load less frequently (fewer days per year) than reaches with finer sediment. However, they also found that differences in transport frequency were offset by differences in transport intensity, such that the total bed load carried through high- and low-gradient reaches was approximately the same. Additional research emphasizing the time-integrated behavior of both fine and coarse sediment would help clarify many of the practical and theoretical questions concerning bed load transport in high gradient channels.

Conclusions

The results presented in this paper indicate that the separation between surface-layer and substrate grain sizes in gravel bed rivers diminishes downstream as the shear stress through the channel network decreases. The substrate is consistently

DOI: 10.1002/esp

much finer than the surface layer, and it has a broader distribution of grain sizes; however, the individual size fractions of the substrate tend to cluster more tightly around average values than the surface, thus the association between grain size and network location is not as evident in the substrate as it is in the surface layer. We find, for example, that 80% of the substrate samples have a median grain size, D_{50s}, in the range of 16–32 mm (a 1 ψ interval), and that, overall, there is no correlation between D_{50s} and reach-average shear stress, τ. In contrast the surface D_{50} is strongly and positively correlated to τ, thus the ratio of surface to substrate D_{50} varies systematically with reach-average shear stress, reflecting a tendency for the channels investigated to become less armored downstream.

The conceptual transport model developed in light of these observations suggests that downstream trends in the total bed load flux through a gravel river system may vary appreciably, depending on the assumed relation between surface-layer and substrate grain sizes. In the two scenarios considered, the channel with a constant ratio of substrate–surface D_{50} carries more bed load in its headwater reaches than the channel with greater armoring and a variable ratio of substrate–surface D_{50}. In downstream reaches, conditions reverse and the channel with a variable surface–substrate D_{50} ratio then carries the higher load due to decreased armoring. The crossover in system behavior appears to reflect differences in the mobility of sediment supplied from the substrate, and the extent to which the bed surface hinders the movement of these finer grains.

Acknowledgements

Portions of this work have been funded by the US Fish and Wildlife Service, the US Forest Service and the National Science Foundation. Numerous people assisted in collecting the field data, including Jillian Aldrin, Brent Barkett, Aaron Cloud, Cherie Cornell, Ingrid Corson, Lex Ivey, Jane Jones, David Lewis, Jennifer Nissenbaum, Janeen Pesiridis, Rebecca Thomas, Mark Van Steeter and Casey Ward. Rob Ferguson and Marwan Hassan provided thoughtful comments that led to significant improvements in the structure and clarity of the manuscript.

References

Andrews ED. 1984. Bed-material entrainment and hydraulic geometry of gravel-bed rivers in Colorado. *Geological Society of America Bulletin* **95**: 371–378.

Andrews ED. 1994. Marginal bed load transport in a gravel bed stream, Sagehen Creek, California. *Water Resources Research* **30**: 2241–2250.

Andrews ED, Erman DC. 1986. Persistence in the size distribution of surficial bed material during an extreme snowmelt flood. *Water Resources Research* **22**: 191–197.

Brummer CJ, Montgomery DR. 2003. Downstream coarsening in headwater channels. *Water Resources Research* **39**: 1294. DOI: 10.1029/2003WR001981

Church M, Ham D. 2004. *Atlas of the Alluvial Gravel-Bed Reach of Fraser River in the Lower Mainland Showing Channel Changes in the Period 1912–1999*. Department of Geography University of British Columbia. http://www.geog.ubc.ca/fraserriver/publications.html [accessed 27 September 2007].

Church M, McLean DG, Wolcott JF. 1987. River bed gravels: sampling and analysis. In *Sediment Transport in Gravel-Bed Rivers*, Thorne CR, Bathurst JC, Hey RD (eds). Wiley: New York; 43–88.

Cinotto PJ. 2003. *Development of Regional Curves of Bankfull-Channel Geometry and Discharge for Streams in the Non-Urban, Piedmont Physiographic Province, Pennsylvania and Maryland*, US Geological Survey Water Resources Investigations Report 03-4014.

Clayton JA, Pitlick J. 2007a. Spatial and temporal variations in bed load transport intensity in a gravel bed river bend. *Water Resources Research* **43**, W02426. DOI: 10.1029/2006WR005253

Clayton JA, Pitlick J. 2007b. Persistence in the surface texture of a gravel-bed river during a large flood. *Earth Surface Processes and Landforms* in press. DOI: 10.1002/esp.1567

Dade WB, Friend PF. 1998. Grain-size, sediment-transport regime, and channel slope in alluvial rivers. *Journal of Geology* **106**: 661–675.

Dietrich WE, Kirchner JW, Ikeda H, Iseya F. 1989. Sediment supply and the development of the coarse surface layer in gravel-bedded rivers. *Nature* **340**: 215–217.

Emmett WW. 1975. *The Channels and Waters of the Upper Salmon River Area, Idaho*, US Geological Survey Professional Paper 870-A.

Emmett WW, Wolman MG. 2001. Effective discharge and gravel-bed rivers. *Earth Surface Processes and Landforms* **26**: 1369–1380.

Ferguson RI. 2003. Emergence of abrupt gravel to sand transitions along rivers through sorting processes. *Geology* **31**: 159–162.

Ferguson RI, Church M, Weatherly H. 2001. Fluvial aggradation in Vedder River: testing a one-dimensional sedimentation model. *Water Resources Research* **37**: 3331–3347.

Ferguson RI, Hoey T, Wathen S, Werritty A. 1996. Field evidence for rapid downstream fining of river gravels through selective transport. *Geology* **24**: 179–182.

Ferguson RI, Paola C. 1997. Bias and precision of percentiles of bulk grain size distributions. *Earth Surface Processes and Landforms* **22**: 1061–1077.

Gasparini NM, Tucker GE, Bras RL. 1999. Downstream fining through selective particle sorting in an equilibrium drainage network. *Geology* **27**: 1079–1082.

Gasparini NM, Tucker GE, Bras RL. 2004. Network-scale dynamics of grain-size sorting: implications for downstream fining, stream-profile concavity, and drainage basin morphology. *Earth Surface Processes and Landforms* **29**: 401–422.

Gomez B, Rosser BJ, Peacock DH, Hicks DM, Palmer JA. 2001. Downstream fining in a rapidly aggrading gravel bed river. *Water Resources Research* **37**: 1813–1823.

Hassan MA, Egozi R, Parker G. 2006. Experiments on the effect of hydrograph characteristics on vertical grain sorting in gravel bed rivers. *Water Resources Research* **42**: W09408. DOI: 10.1029/2005WR004707

Hoey TB, Ferguson RI. 1994. Numerical simulation of downstream fining by selective transport in gravel bed rivers: model development and illustration. *Water Resources Research* **30**: 2251–2260.

Hoey TB, Ferguson RI. 1997. Controls of strength and rate of downstream fining above a river base level. *Water Resources Research* **33**: 2601–2609.

Jones ML, Seitz HR. 1980. *Sediment Transport in the Snake and Clearwater Rivers in the Vicinity of Lewiston, Idaho*, USGS Open-File Report 80-690.

King JG, Emmett WW, Whiting PJ, Kenworthy RP, Barry JJ. 2004. *Sediment Transport Data and Related Information for Selected Coarse-Bed Streams and Rivers in Idaho*, General Technical Report RMRS-GTR 131, USDA Forest Service, Rocky Mountain Research Station. Data from USFS Boise Adjudication Team website: www.fs.fed.us/rm/boise/research/watershed/BAT [accessed 27 September 2007].

Kirchner JW, Finkel RC, Riebe CS, Granger DE, Clayton JL, King JG, Megahan WF. 2001. Mountain erosion over 10-year, 10,000-year, and 10,000,000-year timescales. *Geology* **29**: 591–594.

Kuhnle RA, Willis JC. 1992. Mean size distribution of bed load on Goodwin Creek. *Journal of Hydraulic Engineering* **118**: 1443–1446.

Lisle TE. 1995. Particle size variations between bed load and bed material in natural gravel bed channels. *Water Resources Research* **31**: 1107–1118.

Martin Y, Church M. 1995. Bed-material transport estimated from channel surveys: Vedder River, British Columbia. *Earth Surface Processes and Landforms* **20**: 347–361.

Milhous RT. 1973. *Sediment Transport in a Gravel-Bottomed Stream*, PhD Dissertation, Oregon State University.

Mueller ER, Pitlick J. 2005. Morphologically based model of bed load transport capacity in a headwater stream. *Journal of Geophysical Research-Earth Surface* **110**: F02016. DOI: 10.1029/2003JF000117

Mueller ER, Pitlick J, Nelson JM. 2005. Variation in the reference Shields stress for bed load transport in gravel-bed streams and rivers. *Water Resources Research* **41**: W04006. DOI: 10.1029/2004WR003692

Parker G. 1979. Hydraulic geometry of active gravel rivers. *Journal of the Hydraulics Division ASCE* **105**: 1185–1201.

Parker G. 1990. Surface-based bedload transport relation for gravel rivers. *Journal of Hydraulic Research* **28**: 417–436.

Parker G, Klingeman PC, McLean DB. 1982. Bedload size distribution in paved gravel-bed streams. *Journal of the Hydraulics Division American Society of Civil Engineers* **108**(HY4): 544–571.

Parker G, Wilcock PR, Paola C, Dietrich WE, Pitlick J. 2007. Physical basis for quasi-universal relations describing bankfull hydraulic geometry of single-thread gravel-bed rivers. *Journal of Geophysical Research-Earth Surface* in press. DOI: 10.1029/2006JF000549

Pitlick J, Cress R. 2002. Downstream changes in the channel geometry of a large gravel bed river. *Water Resources Research* **38**: 1216. DOI: 10.1029/2001WR000898

Pitlick J, Van Steeter MM. 1998. Geomorphology and endangered fish habitats of the Upper Colorado River 2: Linking sediment transport to habitat maintenance. *Water Resources Research* **34**: 303–316.

Pitlick J, Van Steeter M, Cress R, Barkett B, Franseen M. 1999. *Geomorphology and Hydrology of the Colorado and Gunnison Rivers and Implications for Habitats Used by Endangered Fishes*, final report. US Fish and Wildlife Service: Grand Junction Colorado. 55pp.

Powell DM, Reid I, Laronne JB. 2001. Evolution of bed load grain size distribution with increasing flow strength and the effect of flow duration on the caliber of bed load sediment yield in ephemeral gravel bed rivers. *Water Resources Research* **35**: 1463–1474.

Ryan SE, Emmett WW. 2002. *The Nature and Flow of Sediment Transport in Little Granite Creek near Bondurant, Wyoming*, USDA Forest Service General Technical Report RMRS-GTR 90S.

Torizzo M, Pitlick J. 2004. Magnitude–frequency of bed load transport in mountain streams in Colorado. *Journal of Hydrology* **290**: 137–151.

Wathen SJ, Ferguson RI, Hoey TB, Werritty A. 1995. Unequal mobility of gravel and sand in weakly bimodal river sediments. *Water Resources Research* **31**: 2087–2996.

Whiting PJ, Stamm JF, Moog DB, Orndorff RL. 1999. Sediment transporting flows in headwater streams. *Bulletin of the Geological Society of America* **111**: 450–466.

Wilcock PR, Crowe JC. 2003. Surface-based transport model for mixed-size sediment. *Journal of Hydraulic Engineering* **129**: 120–128.